



# The influence of the instabilities in modelling arteriovenous junction haemodynamics



Stephen P. Broderick<sup>a</sup>, J. Graeme Houston<sup>b</sup>, Michael T. Walsh<sup>a,\*</sup>

<sup>a</sup> Centre for Applied Biomedical Engineering Research, Department of Mechanical Aeronautical & Biomedical Engineering and Material Surface Science Institute, University of Limerick, Limerick, Ireland

<sup>b</sup> Cardiovascular and Diabetes Medicine, Ninewells Hospital and Medical School, University of Dundee, Dundee, United Kingdom

## ARTICLE INFO

### Article history:

Accepted 30 July 2015

### Keywords:

Computational fluid dynamics  
Arteriovenous junction  
Wall shear stress  
Turbulence  
Instabilities  
Large eddy simulation

## ABSTRACT

The arteriovenous junction is characterised by high flow rates, large pressure difference and typically a palpable thrill or audible bruit, associated with turbulent flow. However, the arteriovenous junction is frequently studied with the assumption of streamline flow. This assumption is based on the Reynolds number calculation, although other factors can contribute to turbulent generation. In this study, the presence of instabilities is examined and the influencing factors discussed. This was performed using a pseudo-realistic geometry with adapted graft angles, vein diameter, outflow split ratio and graft inlet velocity values. Correlation was performed between steady and unsteady averaged simulation cases with correlation performance ranked. Overall the arteriovenous junction is capable of possessing highly disturbed flows, in which strict modelling requirements are necessary to capture such instabilities and avoid erroneous conclusions. Vein diameter and flow split ratio contribute to turbulent generation, thus Reynolds number cannot be used as a sole turbulent criterion in the arteriovenous junction.

© 2015 Elsevier Ltd. All rights reserved.

## 1. Introduction

Arteriovenous junctions (AVJs) are artificial connections between arterial and venous networks that facilitate haemodialysis in chronic kidney disease patients. By surgically connecting arterial and venous networks, either using native vessels (arteriovenous fistulas (AVF)), or with synthetic substitutes (arteriovenous grafts (AVG)), secondary vessels are bypassed producing a large pressure difference across the AVJ and inducing the increased flow rates required for successful haemodialysis. However, AVJs suffer from complications that hinder the functionality of haemodialysis. The most common complications are maturation failure leading to insufficient flow rates and intima-medial thickening (IMT) in the juxta-anastomosis and draining vein.

The mechanisms of maturation and IMT in the AVJ are highly influenced by the induced flow conditions. Arterial and venous flows can increase 10 and 20 fold their respective normal values immediately after creation of the AVJ (Albayrak et al., 2007). This leads to vascular remodelling via endothelial response to wall shear stress (WSS), vasodilatation and pressure induced stress in the wall (Corpataux et al., 2002; Ene-Iordache et al., 2003; Rajabi-Jagahrgoh et al., 2013). Several metrics have been used to quantify

and predict maturation/IMT, from high WSS (Hofstra et al., 1995), low WSS and oscillatory shear index (OSI) (Ene-Iordache and Remuzzi, 2012; Kharboutly et al., 2007), time averaged WSS (Rajabi-Jagahrgoh et al., 2013), time averaged WSS gradient (He et al., 2013), WSS gradient (van Tricht et al., 2006) and vein tissue vibration (Arslan et al., 2005; Lee et al., 2005). Flow in AVJs is generally solved with the assumption of laminar flow phenomena, which is characterised by streamlines, often steady or periodic and the absence of small flow features, allowing model simplifications such as a relaxation on mesh and time-step size. This assumption is based primarily on flow being below a critical Reynolds number (Beasley and Conrad, 2007; Carroll et al., 2011; He et al., 2013; Krishnamoorthy et al., 2008; Sigovan et al., 2013; van Tricht et al., 2006). While quoted Reynolds numbers may be below the critical range of 2000–2300 for sustained turbulent generation (Valen-Sendstad et al., 2013), the AVJ is often described as possessing an audible bruit or palpable thrill (Murphy et al., 2000), a characteristic associated with kinetic energy from disturbed flow (Arslan et al., 2005). However, the presence of disturbed flow has been studied in cases below this threshold. Varghese et al. (2007a) examined geometries with concentric and eccentric stenosis and disturbed flow was found in Reynolds numbers 1000 and as low as 500 in the eccentric case. Lee et al. (2007) examined the AVG model finding an increased tendency for transitional and turbulent flow with flow split at low Reynolds numbers (800–1000). Valen-Sendstad et al. (2013) found the presence of high-frequency

\* Corresponding author.

E-mail address: [Michael.Walsh@UL.ie](mailto:Michael.Walsh@UL.ie) (M.T. Walsh).

velocity fluctuations in intracranial aneurysms, with Reynolds numbers ranging from approximately 200 to 400 dependent on the geometric parameter of aneurysm configuration.

Few studies have examined AVJs using higher order models capable of resolving high fluctuations and instabilities (Lee et al., 2005; McGah et al., 2013) as the computational expense is still prohibitive for large scale pulsatile studies. However, since disturbed and high frequency flow were present in all of those studies, the use of a large mesh and time-step may lead to incorrect flow field and WSS predictions, and thus may alter conclusions based on WSS metrics. This poses the following questions: can the AVJ be described as having highly disturbed flow characteristics? If such characteristics exist, what factors influence the generation of the instabilities in the AVJ. Therefore, the objective of this study is to perform CFD analysis with parameter variations specific to an AVJ under both a steady Navier–Stokes and unsteady large eddy simulation (LES) approach. The presence of highly disturbed flow is to be investigated by measuring the diverging solutions between the steady and unsteady case solutions.

## 2. Methods

### 2.1. Variable parameter selection

Variable selection consisted of both geometric alteration and boundary condition changes. The geometric parameters considered here are the venous diameter, the graft in-plane and out-of-plane angles. The parameter locations are illustrated in Fig. 2(a). The inlet Reynolds number and the flow split ratio are labelled as 'A' and 'E' respectively. The flow split is defined as the ratio between the distal venous segment (DVS) and the proximal venous segment (PVS). The ratios indicate the percentage of the inlet flow exiting the respective boundaries. The convention is positive for flow exiting and negative for flow entering the outlets. All parameter values are displayed in Table 1. Case name convention is described as

#### Diameter\_In plane angle\_Planar/Non – Planar\_flow – split\_Reynolds number

For example, a case with a 4 mm diameter venous section, at an in-planar angle of 15° and an out-of-plane angle of 20°, a flow split of -10:110 and a Reynolds number of 1500 would be described as:

4\_15\_NP\_10110\_1500

With five parameters and the variations for each parameter, a total of 48 cases are possible. By utilising a two-level four-factor half factorial design pattern, the number of cases was reduced to half. This exercises the sparsity-of-effects principle, the highest order effects are assumed not to be dominant and thus can be ignored.

### 2.2. Geometric construction

The geometry was adapted from the venous anastomosis in a canine model, described by Lee et al. (2005). Utilising the structured grid model from various projections, the geometry in Fig. 2(a) was regenerated by nodal point triangulation. A skeleton structure was generated to adapt the geometric parameters outlined in Fig. 2(a). A weighting function was applied between the individual bones and the respective vertices using a linear blend skinning method. Utilising this skeleton, the diameter and graft angle were altered to satisfy the parameters in Table 1.

### 2.3. Mesh

All geometries were meshed using ANSYS ICEM CFD v13.0 (Ansys, Canonbury, P.A., USA). As shown in Fig. 2(b), a structured hexahedral mesh with element density weighted radially to the wall and axial element density increased at the anastomosis and in the proximal venous segment. Cell size distribution is weighted axially finer at the junction and in the proximal venous segment. The largest cell within the junction core is  $0.46 \times 0.15 \times 0.15$  mm, with the largest dimension along the approximate axial direction. A mesh total of approximately 1.6 million cells was applied using a common blocking framework. This framework was changed to fit each geometric alteration and maintained cell count and mesh density between geometries. The mesh was validated by comparison to the DNS data from the works of Lee et al. (2005). There was a strong trend agreement seen in the mean velocities and mean WSS magnitude between cases, with an average percentage error in mean WSS within 7% over the venous segment. In Fig. 1 the normalised time-averaged wall shear stress is illustrated. Visually a good agreement is present between both pairs. Features are commonly recognised between the DNS and LES. However the LES overestimates the peak WSS and sharp contours are not as prominent in the LES. This is to be expected as

**Table 1**  
Summary of parameter labels from Fig. 2(a) with description and values for each parameter.

Label	Description	Variable names
A	Graft inlet Reynolds number	1000, 1500, 2000
B	Out of plane angle	0°, 20° (planar/non-planar)
C	In plane angle	15°, 27°
D	Venous segment diameter	4 mm, 8 mm
E	Flow split ratio of DVS:PVS	30:70, –10:110

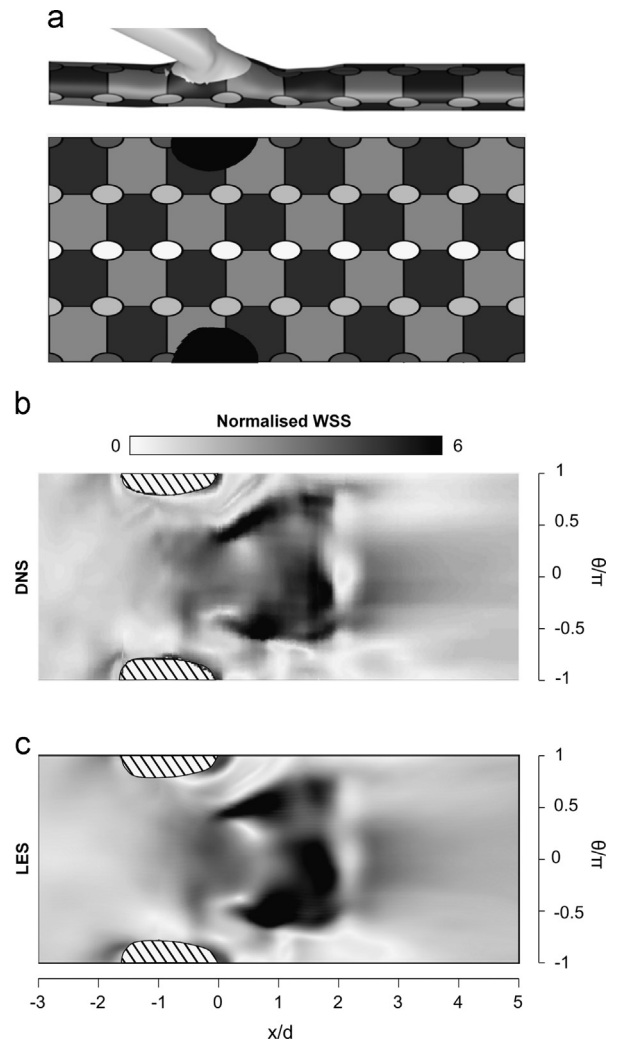


**Fig. 1.** Mean wall shear stress comparison of the unwrapped venous vessel. Shown is the unwrapping illustration (a), the DNS data from Lee et al. (2005) (b) and the reproduced LES data (c). WSS is normalised by the graft inlet WSS, calculated by Poiseuille's law.

spatial resolution in DNS cases is significantly higher. Given the derivative nature of WSS calculation and the inherent limitations between DNS and LES cases, the results displayed in Fig. 1 illustrate a satisfactory mesh and case setup procedure. This result was deemed satisfactory for validation purposes.

### 2.4. Computational analysis

The 3D Navier–Stokes equations are solved using ANSYS Fluent. Pressure–velocity coupling was performed under the SIMPLEC algorithm. Transient formulation was solved under second order implicit time integration. Spatial terms in the Navier–Stokes equations include the pressure and momentum terms. Pressure was discretised as a second order function. Momentum was discretised using the QUICK approach for the steady and bounded central difference for the unsteady cases. The subgrid scale model used was the dynamic Smagorinsky–Lilly model. A secondary filter is utilised to calculate the Smagorinsky constant over the control volume. This model vanishes at

Download English Version:

<https://daneshyari.com/en/article/871861>

Download Persian Version:

<https://daneshyari.com/article/871861>

[Daneshyari.com](https://daneshyari.com)